이동표적 검출를 위한 ISAR 데이터의 인코히어런트 프로세싱

정회원 양 훈 기*

Incoherent Processing of ISAR data for Moving Targets' Detection

Hoon-Gee Yang* *Regular Member*

요 약

본 논문은 SNR이 상당히 낮은 ISAR 데이타로 부터 인코히어런트한 처리를 거쳐 이동표적을 효과적으로 검출할 수 있는 방법을 제시한다. 제시된 방법은 위치와 시간의 함수인 ISAR데이터를 공간주파수 및 시간주파수 함수로 변환한 후 유한개의 시간주파수 함수에서의 공간주파수 함수를 인코히어런트하게 더해줌으로써 이동표적 성분을 검출한다. 주어진 ISAR 시스템 환경에서 수신신호의 공간주파수 평면에서의 대역폭을 제시하며, 인코히어런트하게 더하기 전에 요구되는 전처리과정을 설명한다. 또한 제시된 방법을 구현할 수 있는 zero-padding 방법 및 Nyquist interpolation 방법을 제시하고 각각의 방법에 대한 차이점 및 각 방법에 따른 시뮬레이션 결과를 보인다.

ABSTRACT

An efficient incoherent scheme to detect moving targets' signitures out of heavily corrupted ISAR data is presented. The proposed scheme, converts a received signal in two-dimensional space-time domain into the one in two-dimensional spatial frequency-temporal frequency domain to exploit spatial frequency functions extracted from some specific a finite number of temporal frequencies. In this method, selected spatial frequency functions are incoherently added such that the moving targets' signitures can be detected. The bandwidth of the targets' signitures in the spatial frequency domain are determined and the pre-processing procedure required prior to incoherent addition is described. we present two methods, called zero-padding method and Nyquist interpolation method, to implement the proposed scheme. The differences of these methods are described and the simulation results led by each method are presented.

I. Introduction

Inverse Synthetic Aperture Radar(ISAR) is a coherent imaging method that utilizes the motion of a target to synthesize the effect of a large aperture antenna[1]. For the success of a coherent imaging, the moving target's velocity should be known a priori[2]. In general, the received ISAR data are corrupted by heavy clutter and thus, the estimated velocity is pretty often inaccurate, which degrades the reconstructed image quality[3][4][5]. Recently, we proposed a velocity estimation scheme, called subaperture processing, which is applicable to both SAR and ISAR environment[6]. The proposed scheme could function under a low target-to-clutter ratio(TCR)

In this paper, we propose a detecting scheme of moving targets' signitures under a heavy clutter from ISAR data, which makes possible to filter out the considerable amount of clutter. This in

* 광운대학교 전파공학과 이동통신기술 연구실(hgyang@daisy.kwangwoon.ac.kr), ** 광운대학교
논문번호 : 020212-0503, 접수일자 : 2002년 5월 3일
※ 본 논문은 2001년 광운대학교 교내학술연구비 지원에 의해 연구되었음.

turn enables us to estimate velocity estimation properly. Hence, this method can be viewed as a pre-processing for ISAR imaging. Besides this application, the proposed method itself is valuable as a novel method for moving targets' detection[7]. In Section II, we present a ISAR system model for multiple moving targets and investigate some properties of echoed ISAR signal in spatial frequency domain. In Section III, we present a blind-velocity multiple target detection scheme and examine its feasibility. We next propose two methods to implement the proposed scheme and show simulation results in Section IV and conclusions are followed.

II. ISAR Model with Multiple Moving Targets

Consider a two-dimensional ISAR system geometry on the (x, y) plane as shown in Figure 1. A radar located at (0,0) illuminates the target area with a time dependent pulsed signal $p(t)$ and records the resultant echoed signals. The radar makes such transmissions and corresponding receptions at discrete times of $u \in [-u_0, u_0]$ (we call $2u_0$ data acquisition time) while unknown multiple targets are moving within the radar's footprint. The nth moving target is assumed to have constant velocity $(-A_n, -B_n)$ during the radar's data acquisition time interval, which is plausible in that $2u_0$ is normally short time period. Note that u is a time variable indicating the instant of the pulse transmission while t denotes delay time variable. The targets' coordinates at $u=0$ are denoted by (x_n, y_n). Then, the nth target at time u is located at $(x, y) = (x_n - A_n u, y_n - B_n u)$. For a fixed u, the distance between the radar and the nth target, $R_n(u)$, is

$$R_n(u) = \sqrt{(x_n - A_n u)^2 + (y_n - B_n u)^2}$$

The two-dimensional recorded signal is

$$s_0(u, t) = s_c(t) + \sum_n \frac{g_n}{R_n^2(u)} p[t - \frac{2R_n(u)}{c}] \quad (1)$$

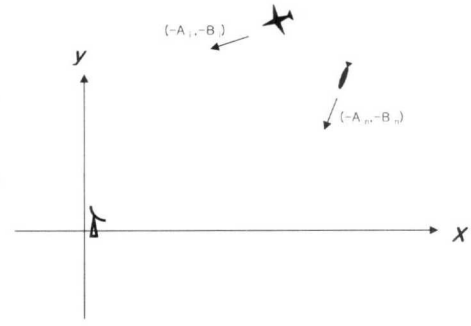

그림 1. 이동 목표물들을 포함하는 시스템 환경

(1) where $s_c(t)$ is the static clutter signature that can be assumed to be invariant of u, c is the propagation speed, g_n is the nth target's reflectance that includes antenna gain and propagation path loss. We model the clutter as an additive white Gaussian noise with variance σ^2. Thus, for a given u, the ratio of the power received from the nth target to the white noise variance is $(S_n/\sigma^2) \approx g_n^2/(R_n^4\sigma^2)$ where $R_n \equiv \sqrt{x_n^2 + y_n^2} = R_n(0)$. Taking the one-dimensional Fourier transform of both sides of (1) with respect to t yields

$$s(u, \omega) \equiv S_c(\omega) + P(\omega) \sum_n g_n \frac{\exp[j2k\sqrt{(x_n - A_n u)^2 + (y_n - B_n u)^2}]}{(x_n - A_n u)^2 + (y_n - B_n u)^2} \quad (2)$$

where ω is radial frequency for t and k is wavenumber defined as ω/c. (2) can be interpreted as a sinario where the nth target is stationary at (x_n, y_n) and

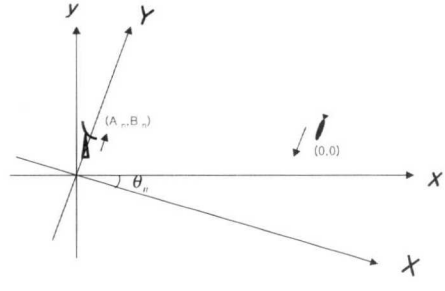

그림 2. 변환된 시스템

the radar moves with velocity vector (A_n, B_n), as illustrated in Fig. 2. We can view this scenario

with respect to a spatial domain (X, Y), which is a θ_n-rotated version of the origianl domain (x, y) where $\theta_n \equiv \arctan(A_n/B_n)$, as follows: a radar moves on Y-axis with speed $V_n \equiv \sqrt{A_n^2 + B_n^2}$, making transmissions and corresponding receptions while a target is stationary, located at (X_n, Y_n) which is defined as

$$\begin{bmatrix} X_n \\ Y_n \end{bmatrix} \equiv \begin{bmatrix} \cos\theta_n & -\sin\theta_n \\ \sin\theta_n & \cos\theta_n \end{bmatrix} \begin{bmatrix} x_n \\ y_n \end{bmatrix}$$

Then, the system model of (2) can be rewritten as

$$s(u, \omega) \equiv S_c(\omega) + P(\omega) \sum_n g_n \frac{\exp[j2k\sqrt{X_n^2 + (Y_n - V_n u)^2}]}{X_n^2 + (Y_n - V_n u)^2}. \tag{3}$$

Taking the Fourier transform on both sides of (3) with respect to $u \in [-u_0, u_0]$ yields[1]

$$S(k_u, w) \equiv S_c(w) \sin c(k_u u_0) + P(\omega) \cdot \sum_n \frac{\alpha_n}{\sqrt{4k^2 - (\frac{k_u}{V_n})^2}} \exp[j\sqrt{4k^2 - (\frac{k_u}{V_n})^2}\, X_n + j\frac{k_u}{V_n} Y_n]\, I_n(k_u) \tag{4}$$

where k_u denote the spatial frequency domain for u, α_n is constant that is the function of g_n, k, u_0 and V_n and $I_n(\cdot)$ is an indicator (band) function defined by

$$I_n(k_u) = \begin{cases} 1 & k_u \in [2k(V_n \sin\theta_n - \frac{u_0 V_n^2 \cos^2\theta_n}{R_n}),\ 2k(V_n \sin\theta_n + \frac{u_0 V_n^2 \cos^2\theta_n}{R_n})] \\ 0 & otherwise \end{cases} \tag{5}$$

where $R_n \equiv \sqrt{X_n^2 + Y_n^2} = \sqrt{x_n^2 + y_n^2}$. Note that the signature of the nth target is centered around

$$H_n = 2kV_n \sin\theta_n = 2kA_n \tag{6}$$

and the bandwidth of this support band is

$$2W_n = \frac{4ku_0 V_n^2 \cos^2\theta_n}{R_n} = \frac{4ku_0 B_n^2}{R_n} \tag{7}$$

in the k_u domain. H_n depends on k (or ω), as illustrated in Fig. 3.

Thus, the following approximations holds for the amplitude function in (4):

$$\frac{\alpha_n}{\sqrt{4k^2 - (\frac{k_u}{V_n})^2}} \approx \frac{\alpha_n}{2kV_n \cos\theta_n} = \frac{\alpha_n}{2kB_n} \tag{8}$$

It is assumed that in the k_u domain, the signature of each target does not overlap with the clutter signature and the signatures of the other targets; i.e.,

$$\begin{cases} I_n(\alpha)\ I_j(\alpha) = 0 & \text{for } all\ j \neq n \text{ and } \alpha \\ I_n(\alpha)\ I_c(\alpha) = 0 & \text{for } all\ n \text{ and } \alpha. \end{cases}$$

where $I_c(\cdot)$ is the support band for the clutter signature. This assumption can be satisfied if each target is moving and its velocity vector is different from each other.

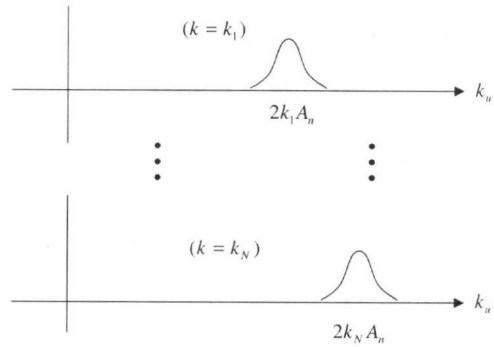

그림 3. k_u 축에서의 스펙트라 분포

To filter out the clutter signature in the k_u domain, we may use a bandstop filter with a rejection band identified by $[-\pi/u_0, \pi/u_0]$. In the following sections, we do not carry the clutter signature, assuming it has been filtered out.

Ⅲ. Target Detection

In section II, we presented the ISAR signal representations in different domains, i.e., $s(u, t)$, $s(u, w)$ and $S(k_u, w)$. To coherently detect moving targets' signiture, we may use a statistic l defined as,

$$\ell(X_n, Y_n, V_n, \phi_n) \equiv |\sum_{k_u} \sum_{\omega} S(k_u, \omega) \exp[-j\sqrt{4k^2 - (\frac{k_u}{V_n})^2}\, X_n - j\frac{k_u}{V_n} Y_n]\, I_n(k_u)|$$

where (X_n, Y_n, V_n, ϕ_n) is the target parameter space. Then, we should find peak valueds for l

via varying parameters (X_n, Y_n, V_n, ϕ_n). This procedure is computationally intensive. The other alternative is, for a given (V_n, ϕ_n), to use the ISAR imaging algorithm to reconstruct the target region. If there were a target with parameters (V_n, ϕ_n), then this target would appear in the reconstructed image. The reconstructed image around the target location should show significantly higher target-to-clutter ratio(TCR) than the TCR in the measurement (u, t) domain. This is due to the fact that the reconstruction algorithm coherently combines the target signature for image formation. However, this process should be repeated for all values of (V_n, ϕ_n) in its prescribed parameter space. Thus, this approach also requires a significant computation time. In the following, we propose a incoherent detection methods that is practical in regard to computation time. The echoed signal due to the nth target can be simply rewritten as (see (4))

$$S(k_u, \omega) = \beta_n(k) \exp[j(\sqrt{4k^2 - (\frac{k_u}{V_n})^2} X_n + j\frac{k_u}{V_n} Y_n)] \; I_n(k_u) \quad (9)$$

where

$$\beta_n(k) \equiv P(\omega) \frac{\alpha_n}{\sqrt{4k^2 - (\frac{k_u}{V_n})^2}}.$$

Under a heavy clutter, i.e., very low TCR, the signal signature at one temporal frequency, whether it is in the u domain or k_u domain, is hardly detectable.

We define the following linear mapping : $h_u \equiv k_u / k$. Then, (9) can be rewritten with respect to h_u by the following:

$$S(k_u, \omega) \equiv Q(h_u, k)$$
$$= \beta_n(k) \exp[jk(\sqrt{4 - (\frac{h_u}{V_n})^2} X_n + j\frac{h_u}{V_n} Y_n)] \; I_n(kh_u). \quad (10)$$

(10) implies that unlike in the k_u domain, the spectral support of the echoed signal in the h_u domain is independent of ω (or k). This means the energy of the echoed signal is centered around $2A_n$ regardless of its frequency component, which is evident in Fig. 6 to appear in Section IV.

Including the presence of Gaussian noise, the echoed signal at wave number k is expressed as follows:

$$Q(h_u, k) = \beta_n(k) \exp[j\xi(k)] \; I_n(kh_u) + n_c(k) + j\, n_s(k)$$

where

$$\xi(k) \equiv k\left(\sqrt{4 - (\frac{h_u}{V_n})^2} X_n + \frac{h_u}{V_n} Y_n\right)$$

and n_c and n_s are real and imaginary components of a complex Guassian noise variable. Here, we assume that they are zero mean Gaussian random variables with variance σ^2. By the proper choice of an orthonormal set, (10) is rewritten as

$$Q(h_u, k) = \beta(k) \; I(h_u) + w_c(k) + jw_s(k) \quad (11)$$

where for notational simplicity, subscript n is dropped in $\beta(k)$ and $I(k)$ and $w_c(k)$ and $w_s(k)$ are two components in a two dimensional vector space formed with a new orthonormal set(see Fig. 4). Note that $w_c(k)$ and $w_s(k)$ are also zero mean Gaussian

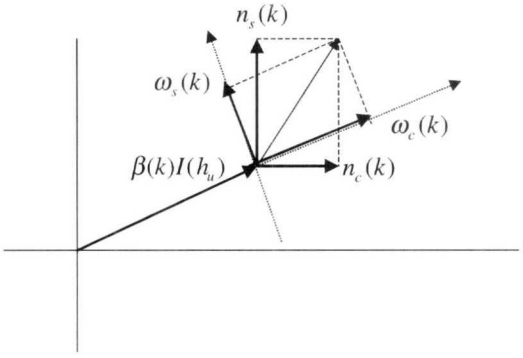

그림 4. 벡터 공간 변환

random variable with a variance σ^2. Now, consider the sum of $|Q(h_u, k_i)|^2$'s obtained at different wavenumber k_i. Using (11), this sum that is normalized with the number of frequency N, is represented by

$$\chi(h_u) \equiv \frac{1}{N} \sum_{i=1}^{N} |Q(h_u, k_i)|^2 = \frac{1}{N} \sum_{i=1}^{N} [z(k_i)^2 + w_s(k_i)^2] \quad (12)$$

where $z(k_i) \equiv \beta(k_i) + w_c(k_i)$. Hence, $z(k_i)$ is a Gaussian random variable with mean $\beta(k_i)$ and variance σ^2. To examine the statistical property for $\chi(h_u)$, we will first find a moment generating function. The moment generating function for $z^2(k_i)$ is

$$\psi_{z^2(k_i)}(t) \equiv E[\exp[z^2(k_i)\rho]]$$
$$= \int \exp[z^2(k_i)\rho] \frac{1}{\sigma\sqrt{2\pi}} \exp[-\frac{(z(k_i)-\beta(k_i))^2}{2\sigma^2}]\, dz(k_i)$$
$$= \frac{1}{\sqrt{1-2\sigma^2\rho}} \exp[\frac{\beta(k_i)^2\rho}{1-2\sigma^2\rho}]$$

where ρ is an independent variable for a moment generating function. The moment generating function for $w_c^2(k_i)$ is, by the same procedure,

$$\psi_{w_c^2(k_i)}(\rho) = \frac{1}{\sqrt{1-2\sigma^2\rho}}.$$

Hence, the resultant moment generating function for $\chi(h_u)$ is expressed as

$$\psi_{\chi(h_u)}(\rho) = \frac{1}{N}(1-2\sigma^2\rho)^{-N} \exp\left[\frac{\rho}{1-2\sigma^2\rho}\left(\sum_{i=1}^{N}\beta^2(k_i)\right)\right] \quad (13)$$

By the property of the moment generating function, the mean and the variance for $\chi(h_u)$ can be found as follows:

$$E[\chi(h_u)] = \frac{d}{dt}\psi_\chi(\rho)|_{\rho=0} = 2\sigma^2 + \lambda$$
$$Var[\chi(h_u)] = \frac{d^2}{dt^2}\psi_\chi(\rho)|_{\rho=0} - (E[\chi(h_u)])^2 \quad (14)$$
$$= \frac{4\sigma^2}{N}(\sigma^2+\lambda)$$

where

$$\lambda \equiv \frac{1}{N}\sum_{i=1}^{N}\beta^2(k_i) \quad (15)$$

To examine the statistical property of λ, we rephrase (15) into

$$\lambda \approx \frac{1}{N}\sum_{i=1}^{N}\left(P(\omega_i)\frac{\alpha_n}{2k_iB_n}\right)^2 \quad (16)$$

To obtain (16), we used (7) and (16). For bandpass signal, $|k_N - k_1| \ll k_1$ holds. Thus, λ is random process with respect to N and does not increase or decrease as N increases. This implies the variance of $\chi(h_u)$ is inversely proportional to N, or, as N increases, a target signature in the $\chi(h_u)$ will gradually become prominent in the region of

$$h_u \in \left[2\left(A_n - \frac{u_0 B_n^2}{R_n}\right), 2\left(A_n + \frac{u_0 B_n^2}{R_n}\right)\right] \text{(see(5) and (6)).}$$

Ⅳ. Simulation Results

First step to implement the proposed algorithm is to modify the received signal in the (k_u, ω) domain into the signal in the (h_u, ω) domain. As shown in Fig.3, the location of the center of gravity of the echoed signal in the k_u domain varies depending on the frequency component. However, it does not depend on the frequency component in the h_u domain. Let Δ be the sample spacing in the k_u domain, which is $\Delta = 2\pi/2u_0$ by the DFT(Discrete Fourier Transform) theory. Then there exist m_i's that meet the equitations 2

$$k_i A_n = \Delta \times m_i \quad (i = 1 \cdots N) \quad (17)$$

where $\Delta \times m_i$ represents the value of k_u that maximizes the amplitude of the frequency component at $\omega = \omega_i$, that is, $|S(k_u, \omega_i)|$. To convert the echoed signal into (h_u, ω) domain, or, to colocate the center of gravities of each frequency component, $m_i s'$ should be the same regardless of k_i, which is mathematically impossible. This problem was tackled by two methods. In the first method, we made the sample spacing Δ vary depending on k_i. Let Δ_i be the desired sample spacing in the k_u domain for $k = k_i$. To make all $m_i s'$ be equal, Δ_i should satisfy $2k_i A_n/\Delta_i = 2k_j A_n/\Delta_j$, which results in

$$\Delta_i/\Delta_j = k_i/k_j \quad (18)$$

, or equivalently,

$$u_i = u_j k_j / k_i \tag{19}$$

because of $\Delta_i = 2\pi/2u_i$ where $2u_i$ denote the desired data acquisition time for $k = k_i$. In reality, $2u_i$ can not be different for different frequency component $s(u, \omega_i)$. Due to the fact that if $k_i < k_j$, then $u_i > u_j$ by (19), we, for convinence, fixed $u_N = u_0$ and other u_is' were calculated by $u_i = u_N k_N / k_i$ (see (19)). As the actual acquisition time is $2u_0$, $s(u, \omega_i)$ should be synthesized by zero-padding, that is,

$$s(u, \omega_i) = \begin{cases} s(u, \omega_i) & \text{for } |u| \le u_0 \\ 0 & \text{for } |u| > u_0 \end{cases} \tag{20}$$

The zero-padding shown in (20) guarantees m_i's in (17) are equal for any frequency components. However, via zero-padding, the number of samples are different for each frequency component. Let M denote the number of pulse transmissions. Then, the number of data samples for $k = k_N$ becomes M. For data samples of the other frequency components, after taking FFT with respect to u and applying the conversion algorithm into (h_u, k), we have only to cut off samples of higher spatial frequencies that exceed the number of sample M. In the following discussion, we call this the zero-padding method. In the second method, we made (18) satisfied by using interpolation rather than by the zero-padding. If $k_i < k_j$, $\Delta_i < \Delta_j$ by (18). Thus, in this method, we set $\Delta_N = \Delta = 2\pi/2u_0$ and determine Δ_i by $\Delta_i = \Delta_N k_i / k_N$. We then interpolated the sample values of $S(m\Delta_i, \omega_i)$ from $S(n\Delta, \omega_i)$ by the following Nyquist interpolation formula

$$S(n\Delta_i, \omega_i) = \sum_{m=-\infty}^{\infty} S(m\Delta, \omega_i) \frac{\sin(\frac{\pi}{\Delta}(n\Delta_i - m\Delta))}{\frac{\pi}{\Delta}(n\Delta_i - m\Delta)} \tag{21}$$

Although the range of $\sum$ is $-\infty$ to ∞, we, by windowing, used 4 to 6 adjacent samples to reduce the computation time. As this method changes the sample spacing in the k_u domain depending on the frequency component, the number of samples are different, as in the zero-padding method. Thus we can remove data samples exceeding M exactly in the same manner as we did in the zero-padding method.

After converting the data in (k_u, k) domain into (h_u, k) domain, we used (13) to calculate $I(h_u)$. System parameter values used in the simulation are as follows: At 1024 discrete time instant within time period of $u \in [0., 2]$ (sec), a radar transmits a sequence of pulses and receives an corresponding echos from two moving targets residing in the radar footprint. Each target is simulated as a point scatterer. Target 1 has a velocity vector (120,170) (m/sec) and is located at (10001,2) (m) when $u = 1$. Target 2 has the velocity vector (60,70) (m/sec) and its location at $u = 1$ is (9970,50) (m). We simulated the echoed signal by (3), where the amplitude of each frequency component $P(\omega)$ is assumed to be constant and we set $g_1 = 2$ and $g_2 = 1$. The simulated data $s(u, \omega_i)$ were calculated at uniformly spaced 256 different frequencies which are in the arbitrarily selected frequency range from 239 MHz to 260 MHz. Fig. 5 shows the amplitude of $S(k_u, k_i)$, in which x-axis specifies k_u domain and y-axis represents k domain. There exist two moving targets' signitures whose centers of gravities and bandwidths are dictated by (6) and (7), respectively. Fig. 6 shows the figure of $|Q(h_u, k)|$ which

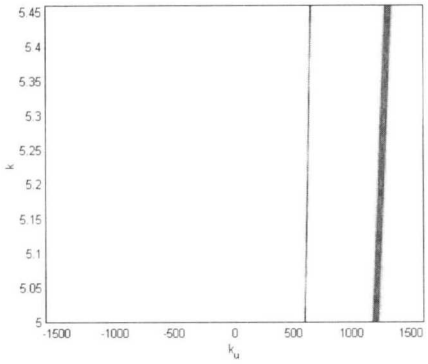

그림 5. $S(k_u, k)$의 진폭

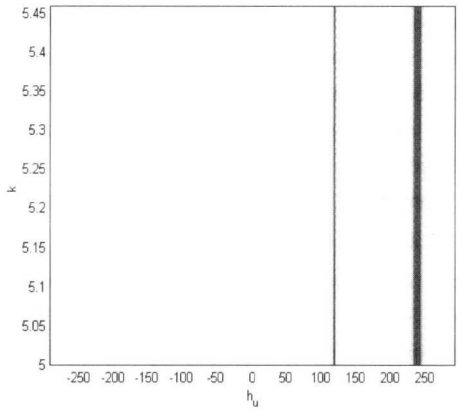

그림 6. $Q(h_u, k)$의 진폭

were obtained from $S(k_u, k)$ by the zero-padding method. The figure of $|Q(h_u, k)|$ obtained by the Nyquist interpolation method is omitted because of its negligible difference from Fig. 6. To see the performances of the proposed scheme, we added Gaussian noise to the echoed signal $s(u, \omega)$ as much as targets' signitares were conpletely embedded in the clutter. We next, via taking Fourier transform and applying the zero-padding method, obtained $Q(h_u, k)$. As the added noise is independent of the echoed signal, it is still uniformly distributed in the (h_u, k) domain(see Fig. 7). Finally using (13), we calculated $\chi(h_u)$. Fig. 8 to 11 show the plots of $\chi(h_u)$ versus h_u, varying the number of terms summed, N. For $N=1$ and even for $N=50$, we can not see targets' signitures. However, when N is significant as much as 100, two targets' signitures are detectable. We next used the Nyquist interpolation method for the noise added data $S(k_u, \omega)$. Fig. 12, Fig. 13 and Fig. 14 show the plots of $\chi(h_u)$ versus h_u for $N=50, 100$ and 200, respectively. The results of the Nyquist interpolation method were almost comparable to those of the zero-padding method. The performances of the Nyquist interpolation method depends on the accuracy of the interpolator. In case of low TCR as in this example, the interpolator is apt to work erroneously. On the other hand, the inaccuracy of the zero-padding

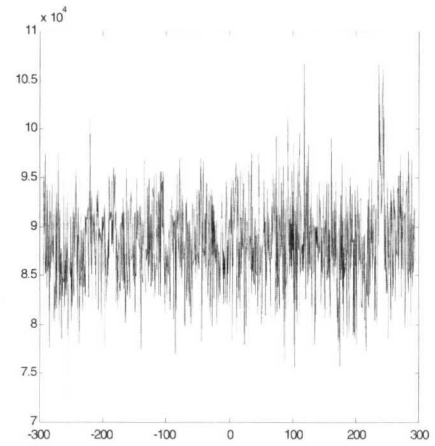

그림 7. N=100인 경우의 $\chi(h_u)$

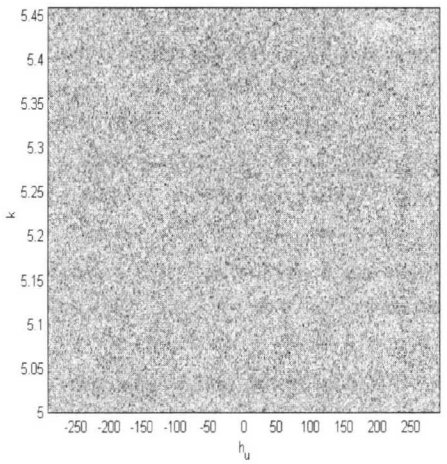

그림 8. $|Q(h_u, k)|$가 더해진 노이즈

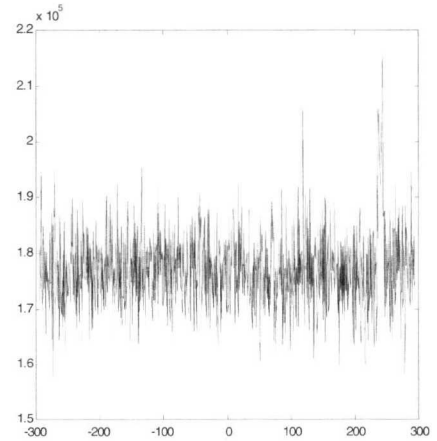

그림 9. N=200인 경우의 $\chi(h_u)$

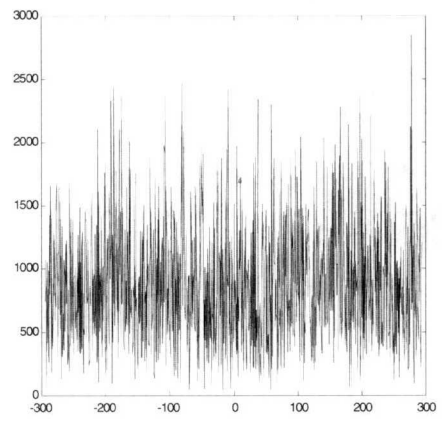

그림 10. N=1인 경우의 $\chi(h_u)$

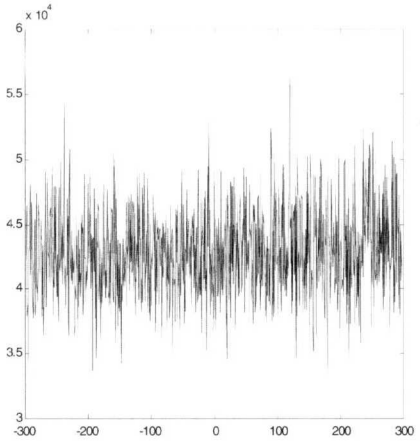

그림 11. N=50인 경우의 $\chi(h_u)$

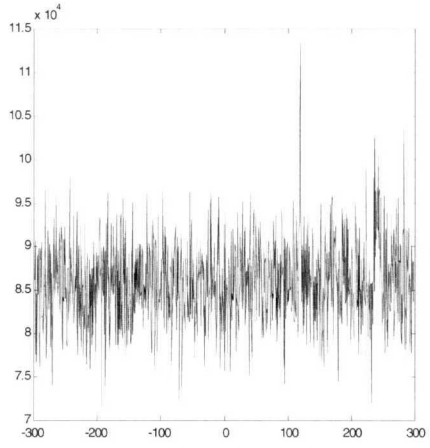

그림 12. N=100인 경우의 $\chi(h_u)$

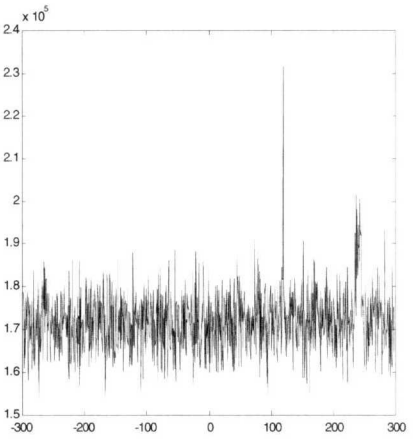

그림 13. N=200인 경우의 $\chi(h_u)$

method lies in the fact that the zero-padded data acquisition time is not integer multiple of pulse repetition period, which is $2u_0/M$. This kind of error is independent of the noise level. Moreover, as the Nyquist interpolatation method requires more computation time, the zero-padding method is more recommandable in low TCR.

V. Conclusions

In this paper, we presented an incoherent method to detect moving targets from the ISAR data corrupted with heavy clutter. The feasibility of the proposed scheme was mathematically proved and we also presented two methods, that is, the zero-padding method and the Nyquist interpolation method, to implement it. Intrinsically, the Nyquist interpolation method should give better results at the expense of complexity. However, due to heavy clutter, which prevents the Nyquist interpolation method from working properly, the outputs from both methods were almost comparable. Through simulation results, the proposed scheme explicitely showed the localized targets' signitures in the linearly mapped spatial frequency domain. Information on the locations of the targets' signitures can be used to filter out the clutter for obtaining ISAR signal of much higher TRC. Further research will

investigate on the usefulness of the proposed scheme for estimating the targets' velocities and imaging the targets.

References

[1] M. Soumekh, "A system model and inversion for synthetic aperture radar imaging," *IEEE Trans. on Image Processing*, vol.1, pp 64-76, January 1992.

[2] R. K. Raney, "Synthetic aperture imaging radar and moving targets," *IEEE Trans. Aerospace and Electronic Systems*, pp. 499-505, May 1971.

[3] S.D. Blostein, T.S. Huang "Detecting Small, Moving Object in Image Sequence Using Sequential Hypothesis Testing," *IEEE Trans. on Signal Processing*,vol. 39, pp. 1611-1629, July 1991.

[4] A. W. Rihaczek, " Radar Resolution of Moving Targets," *IEEE Trans. on Information Theory*, vol. IT-13, pp. 51-56, January 1967.

[5] D.Blacknell, A. Freeman, R. White and J.Wood, "The Prediction of Geometric Distortions in Airborne Synthetic Aperture Radar Imagery from Autofocus Measurements, "*IEEE Trans. Geoscience and Remote Sensing*, 25, p.775, November 1987.

[6] H. Yang, M. Soumekh, "Blind-velocity SAR/ ISAR imaging of moving target in a stationary background," *IEEE Trans. on Image Processing*, vol. 2, pp. 80-95,January 1993.

[7] M.I. Skolnik, *Introduction to Radar Systems*, New York: McGraw-Hill, 1980.

[8] H.L. Van Trees, *Detection, Estimation, and Modulation Theory*, Part III, John Wiley & Sons, pp. 238-243, 1971.

양 훈 기(Hoon-Gee Yang) 정회원

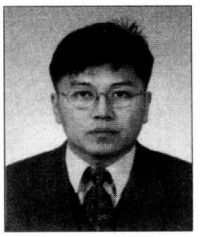

1985년 2월 : 연세대학교 전자공학과 (공학사)
1987년 5월 : SUNY at Buffalo (석사)
1992년 5월: SUNY at Buffalo (박사)

1993년 3월~현재 : 광운대학교전파공학과 교수
<주관심 분야> 레이더 신호처리 광신호처리 통신 및 디지틀 신호처리